Large Quasistatic Magnetic Fields Generated by a Relativistically Intense Laser Pulse Propagating in a Preionized Plasma

M. Borghesi, A. J. Mackinnon, R. Gaillard, and O. Willi
Imperial College of Science, Technology and Medicine, London, United Kingdom

A. Pukhov* and J. Meyer-ter-Vehn
Max-Planck-Institut für Quantenoptik, D-85748 Garching, Germany
(Received 14 November 1997)

Two spatially separated toroidal magnetic fields in the megagauss range have been detected with Faraday rotation during and after propagation of a relativistically intense laser pulse through preionized plasmas. Besides a field in the outer region of the plasma oriented as a conventional thermoelectric field, a field with the opposite orientation closely surrounding the propagation axis is observed, in conditions under which relativistic channeling occurs. A 3D particle-in-cell code was used to simulate the interaction under the conditions of the experiment. [S0031-9007(98)06343-1]

PACS numbers: 52.40.Nk, 52.60.+h, 52.65.–y, 52.70.–m

Applications such as the fast ignition scheme for inertial confinement fusion [1] have generated worldwide interest in the study of the propagation of a relativistically intense laser pulse through plasmas. An important role in the complex interaction between laser radiation and background plasma is expected to be played by the presence of large self-generated quasistatic magnetic fields. It has been demonstrated in several numerical simulations that large magnetic fields can be generated in underdense plasmas [2]. In particular, 2D [3] and, more recently, 3D [4] particle-in-cell (PIC) simulations have shown that, in the relativistic regime, the laser radiation drives strong currents of relativistic electrons in the direction of the light propagation, magnetizing the plasma. The large magnetic fields produced by the fast electron currents can affect the laser propagation, leading to magnetic focusing in addition to the ponderomotive and relativistic self-focusing mechanisms. Propagation in narrow channels has recently been observed in several experiments [5,6]. In particular, an experiment performed by our group [5] indicated that the 1 ps, 1 μm interaction pulse was confined, during its propagation through the plasma, into a channel of a few microns in diameter. 3D PIC simulations used to model the interaction predicted the generation of large magnetic fields by MeV electron currents, through the mechanism described in [4]. Despite the wide interest surrounding the production of magnetic fields in relativistic interactions with preformed plasmas, no experimental measurements have yet been reported.

This paper presents polarimetric measurements of the magnetic fields generated during the interaction of 1–3 ps, 5–10 TW laser pulses with a near critical, underdense preformed plasma. The measurements indicate the presence of two different types of toroidal fields generated during the interaction. In the outer region of the plasma, a magnetic field oriented as a conventional thermoelectric field is observed, whereas close to the laser axis a field with opposite orientation is seen, consistent with generation by an electron current propagating down the short pulse induced channel. The interaction has been modeled using 3D PIC simulations.

The experiment was performed at the Rutherford Appleton Laboratory, using the Vulcan Nd:glass laser in the chirped pulse amplification (CPA) mode. The experimental setup was similar to the one used in [5]. The targets were plastic (CH or Formvar) films with a thickness between 100 and 500 nm. The plasma was preformed by a 400 ps pulse ($\lambda = 0.527\ \mu$m), which was focused onto target, in a spot between 200 and 300 μm in diameter, at an irradiance below 10^{13} W/cm^2. A 1.054 μm, 5–10 TW CPA interaction pulse, 1 to 3 ps in duration, suitably delayed, was focused into the preformed plasma in a 12–15 μm full width at half maximum (FWHM) focal spot, giving an incident irradiance in the range $(3–9) \times 10^{18}$ W/cm^2. The plasma was diagnosed with a temporally independent probe pulse which was split off from the uncompressed interaction beam. The probe beam was compressed by a pair of gratings, frequency doubled in a KDP (potassium dihydrogen phosphate) crystal, and finally Raman shifted in ethanol to $\lambda = 0.622\ \mu$m. Faraday rotation of the optical probe was used to detect the magnetic fields present in the plasma. The spatial resolution determined by the optical system was around 2–3 μm. Time resolved density maps of the plasma were also obtained, using the nonshifted probe and a Nomarski modified interferometer [7].

The interaction stage of the experiment was simulated with the 3D particle-in-cell (PIC) code VLPL (virtual laser plasma laboratory) [4,5]. The PIC code follows the dynamics of about 3×10^7 numerical electrons and 10^7 ions on a $1000 \times 100 \times 100$ spatial mesh during the 1.5 ps interaction time and an additional 0.5 ps after interaction. A plasma layer ($0 < x < x_0$) with the density profile $n = n_0 \exp[(x - x_0)/\Delta p]$ is simulated, setting $\Delta p = 45\ \mu$m and $n_0 = 1.8 \times 10^{20}$ cm^{-3}. This corresponds to the density profile in which the magnetic field was detected experimentally. The longitudinal density gradient is modeled by using particles with different weights, but the same charge-to-mass ratio such that, initially, each cell in the plasma region contains the same number of particles. The incident laser pulse has a Gaussian profile both in transverse and longitudinal direction, a diameter of 12 μm, and a maximum intensity of 5×10^{18} W/cm^2. The simulation has been performed on a 64 processor partition of the CRAY-T3E at Rechenzentrum Garching.

The measurements show that large magnetic fields are generated as a consequence of the interaction of the picosecond pulse with the preformed plasma. No fields were measured when only the heating beam was incident on the target. When the interaction beam was focused into the preformed plasma, two different types of toroidal magnetic fields, with opposite orientation, were detected. Two polarigrams are shown in Fig. 1 which were recorded in separate experiments. The polarigram of Fig. 1(a) was taken during the interaction of a 3 ps, 5 TW pulse, at an irradiance of about 3×10^{18} W/cm^2, with an underdense preformed plasma, while the one of Fig. 1(b) was taken 18 ps after the interaction of a 1.5 ps, 10 TW pulse, at an irradiance of $(6-9) \times 10^{18}$ W/cm^2 with the preformed plasma (the on-axis density profiles of the preformed plasmas are also shown in the figures). The probe duration and the precision in the timing were of the order of the interaction beam duration. Polarizer and analyzer were set 10° off crossed [in the clockwise direction in the case of Fig. 1(a), in the anticlockwise direction in the case of Fig. 1(b)].

In both figures the typical signatures of the presence of a toroidal magnetic field [8], i.e., a dark-bright pattern [darker than the background above the laser propagation axis and brighter below in Fig. 1(a), vice versa in Fig. 1(b)], can be seen in the outer region of the plasma, as far as 100 μm from the laser axis. In Fig. 1(a) a smaller spatial scale dark-bright pattern, with opposite orientation with respect to the outer one and radial extent of about 15–20 μm, is also visible, close to the laser axis, on the edge of the region inaccessible for probing. The bright area enclosed inside the shadowed region is due to self-emission. Also in Fig. 1(b), though the self-emission is partially obscuring the region closer to the laser axis, an inner, inverted rotation pattern can be noticed. The radial extent of the inner pattern is in this case about 30 μm.

The rotation angle inversion is more clearly visible in the lineout of Fig. 2(a) taken along the direction indicated by the arrows in Fig. 1(a). The value of the outer rotation (about 2°) suddenly decreases by almost 3° approaching the laser axis. The corresponding lineout for the product nB, extracted by Abel inversion, is shown in Fig. 2(b). From the plot it is evident that the abrupt changes in rotation angle observed in the data must correspond to an

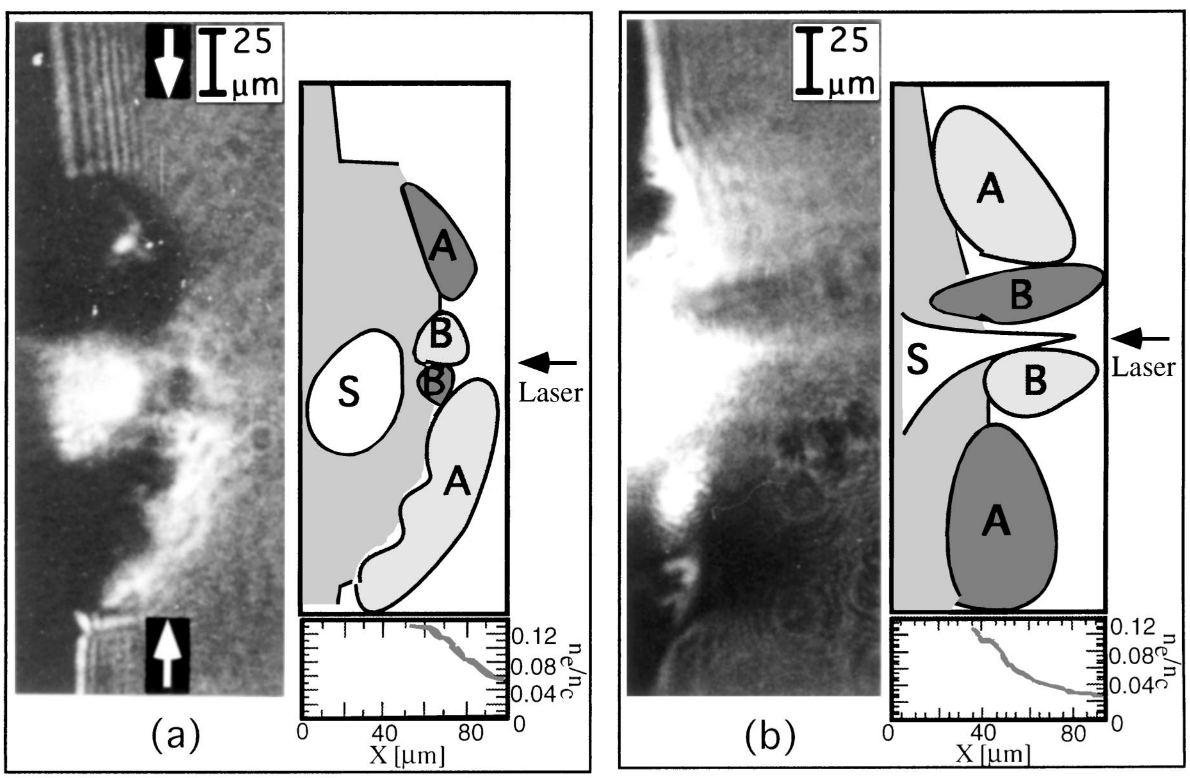

FIG. 1. Polarigrams taken (a) during the interaction of a 3 ps, 5 TW pulse with a preformed plasma (polarizers set −10° off-crossed) and (b) 18 ps after the interaction of a 1.5 ps 10 TW pulse with a preformed plasma (polarizers set +10° off-crossed). The on-axis density profiles of the preformed plasmas are also shown. The schematics indicate the outer (A) and inner Faraday rotation pattern (B), and the regions where self-emission is observed (S).

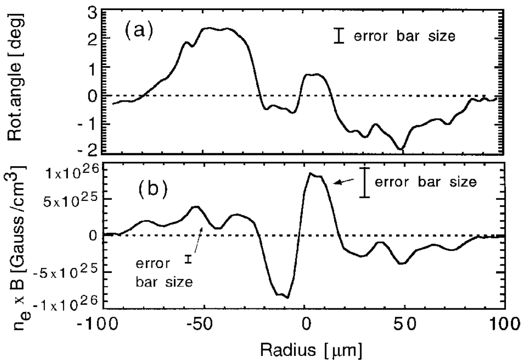

FIG. 2. (a) Faraday rotation angle obtained by microdensitometry along the arrows of Fig. 1(a). (b) Lineout of nB (density times magnetic field) extracted by Abel inversion from the trace of (a).

inversion of the magnetic field direction. A value for the outer magnetic field can be extracted from the corresponding rotation, dividing the product nB by the density n of the preformed plasma. This gives an amplitude of a fraction of 1 MG for Fig. 1(a) and of 1 MG for Fig. 1(b).

In order to better understand the inner magnetic field observations, it is worth remembering here that, as reported in [5], in these experimental conditions the pulse undergoes relativistic self-channeling. An evacuated channel is formed during the interaction due to the combined effect of ponderomotive expulsion of the electrons and subsequent motion of the ions due to the strong space-charge field. Even after the laser pulse is turned off, the channel structure still expands. The evolution of the channel radius with time, as measured interferometrically in the experimental conditions of [5] (i.e., close to those of the polarigrams presented above) is shown in Fig. 3. As also visible in Fig. 3 the expansion is described very well by the function $R(t) = K(t - t_0)^{1/2}$. This is the self-similar analytical solution for a cylindrical blast wave (with K a constant of the order of $(E_0/\rho_0)^{1/4}$, where E_0 is the energy deposited in the plasma per unit length and ρ_0 the unperturbed density) [9], with the time axis shifted by $t_0 = 1.8$ ps. The shift t_0 is comparable with the temporal uncertainty of the measurements. Also, it is reasonable to assume that the similarity solution does not hold in the first picoseconds, when the plasma has not yet reached local thermal equilibrium. By fitting the data with the function above, the energy deposited in the channel results to be in the order of $E_0/\rho_0 \approx 5$ (J/μm)/(g/cm^3). By integrating E_0/ρ_0 over a typical experimental density profile, the total energy deposited along the channel is therefore estimated to be about 0.5 J. Finally, it is interesting to observe that the radial extent of the inner Faraday rotation detected in the experiment appears to be coincident with the channel radius size at the time of observation, suggesting that the magnetic field stays confined within the channel walls during the channel expansion.

The amplitude of the field inside the channel can be estimated, for Fig. 1(a), as $B[\mathrm{MG}] = (n_{\mathrm{in}}/n_0)$ where n_{in} is the density inside the channel and n_0 is the background density of the preformed plasma. Values in the range 5–10 MG are obtained if one considers n_{in} to be of the order of $(0.1-0.5)n_0$ (values reasonably assumable from the experimental observations).

The direction of the outer field is consistent with generation via the $\nabla n \times \nabla T$ mechanism [8] (i.e., also consistent with a current of electrons ejected from the focal spot toward the laser and flowing back into the plasma outside the focal spot region). Indeed, the plasma can be heated up even far away from the laser axis, e.g., due to electrons accelerated under some angle to the pulse propagation by transverse-wake wave breaking processes [10]. The field of opposite direction detected around the laser axis is consistent with the generation mechanism described in [3,4], i.e., with a current of fast electrons traveling on axis together with the laser pulse and spatially separated return currents.

The interaction was studied, under conditions close to those of the reported experiment, using the 3D PIC code VLPL [4]. The 3D simulation results after 2 ps are presented in Fig. 4. The characteristic features of the code output are the same as reported in [5]. A large toroidal

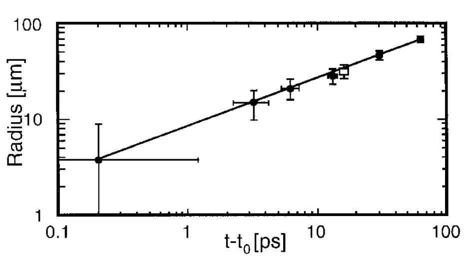

FIG. 3. Temporal evolution of the channel radius in the plasma (solid circles). The temporal axis is shifted by $t_0 = 1.8$ ps. The solid line represents the best fit of the data using the function $R = K(t - t_0)^{0.5}$. The spatial extent of the inner magnetic field in the polarigram of Fig. 1(b) is also shown (empty square).

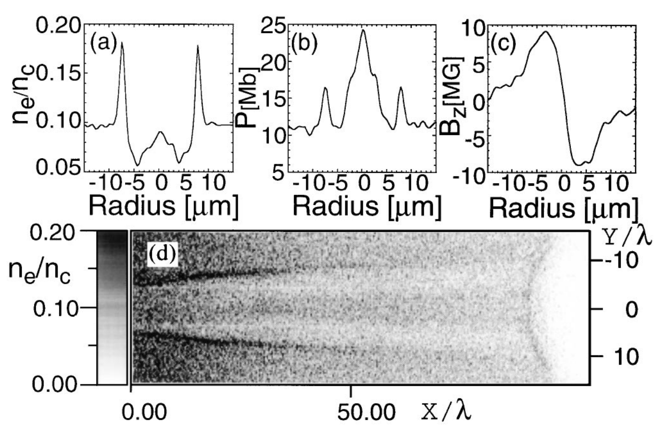

FIG. 4. 3D PIC code prediction. (a)–(c): Radial lineout at a background density of $0.1n_c$ after 2 ps for (a) density, (b) pressure, and (c) magnetic field. (d) Longitudinal 2D section of the electron density.

magnetic field surrounding the laser axis is observed, in correspondence with a current of relativistic electrons traveling with the laser pulse. At a background density of $0.1n_c$, as it can be seen in Fig. 4(c), the magnetic field is predicted to be as large as 9 MG, peaking at a distance of 4–5 μm from the laser axis. In the predicted density profile, one observes that the beam has formed a hollow cylinder type of depression, with outgoing shocks and a density maximum on axis. Such a ringlike filamentation, already reported in [4], is further shown in the 2D longitudinal section in Fig. 4(d). It is interesting to observe that the predicted value of the magnetic field is consistent with the experimental observation of Fig. 1(a) assuming a channel density of 10% of the background density. It can also be seen from Fig. 4 that the peak of the magnetic field coincides with the region of maximum cavitation.

Indeed, a density peak on axis, as predicted by the PIC code, is consistent with some of the experimental observations. In Fig. 5 an interferogram taken 5 ps after the interaction is shown, in which a density increase (up to a few times the background density of $n_c/10$) can be inferred from the fringe shift at the center of the channel. Under certain conditions, the density spike may be enhanced by magnetic pinching after the end of the pulse, and could have significant consequences on the propagation of a second pulse along the channel.

In conclusion, toroidal magnetic fields generated during the interaction of 1–3 ps, 5–10 TW pulses with preformed underdense plasmas have been detected using a polarimetric technique. A large scale magnetic field (in the order of MG), with orientation compatible with thermoelectric generation mechanism, and a magnetic field, estimated to be in the range of 1–10 MG, with opposite orientation and smaller spatial scale, appear to be generated as a consequence of the interaction, as the pulse channels itself through the plasma. The subsequent channel expansion is well described by the self-similar solution for a cylindrical blast wave. 3D PIC simulations were used to model the inner field generation in conditions similar to the experiment, suggesting that the field is produced by a current of relativistic electrons traveling with the laser pulse.

The authors would like to acknowledge the support received by the staff of the Central Laser Facility (Rutherford Appleton Laboratory). This work was funded by an EPSRC/MOD grant. One of the authors (A. J. M.) was supported by a Lawrence Livermore National Laboratory contract.

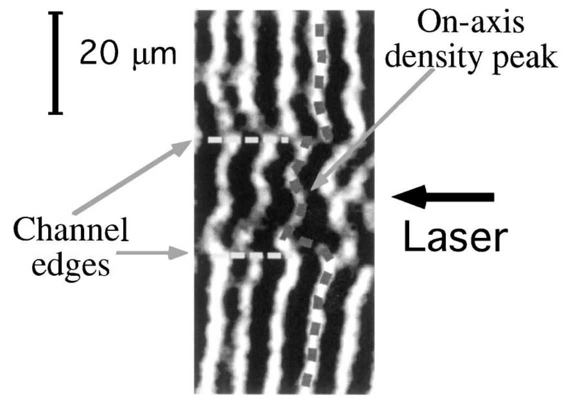

FIG. 5. Detail of an interferogram taken 5 ps after the interaction, in the conditions of Fig. 1(b). The positive fringe shift at the center of the channel is consistent with a density peak on axis.

*On leave from Moscow Institute for Physics and Technology, Dolgoprudny, 141700, Russia.
[1] M. Tabak *et al.*, Phys. Plasmas **1**, 1626 (1994).
[2] L. Gorbunov, P. Mora, and T. M. Antonsen, Jr., Phys. Rev. Lett. **76**, 2945 (1996); S. V. Bulanov *et al.*, Phys. Rev. Lett. **76**, 3562 (1996).
[3] S. V. Bulanov, F. Pegoraro, and A. M. Pukhov, Phys. Rev. Lett. **74**, 710 (1995); G. A. Askar'yan *et al.*, JETP Lett. **60**, 251 (1994).
[4] A. Pukhov and J. Meyer-ter-Vehn, Phys. Rev. Lett. **76**, 3975 (1996).
[5] M. Borghesi *et al.*, Phys. Rev. Lett. **78**, 879 (1997).
[6] P. E. Young and R. Bolton, Phys. Rev. Lett. **77**, 4556 (1996).
[7] R. Benattar, C. Popovics, and R. Sigel, Rev. Sci. Instrum. **50**, 1583 (1979).
[8] J. A. Stamper, Laser Part. Beams **9**, 841 (1991).
[9] L. I. Sedov, *Similarity and Dimensional Methods in Mechanics* (Academic Press, NY, 1959), pp. 210–230.
[10] S. V. Bulanov *et al.*, Phys. Rev. Lett. **78**, 4205 (1997).